PHYSICAL REVIEW A **89**, 052501 (2014)

He$^-$ in a magnetic field: Structure and stability

J. A. Salas and K. Varga
Department of Physics and Astronomy, Vanderbilt University, Nashville, Tennessee 37235, USA

(Received 22 January 2014; revised manuscript received 3 March 2014; published 1 May 2014)

The energy of the He$^-$ ion in a magnetic field is calculated using the stochastic variational method with a deformed correlated Gaussian basis. The energy levels and the stability domains are calculated and the accuracy of the approach is shown by comparison to previous calculations. The structure of these states is studied by calculating the electron-electron and electron-nucleus distances. In the weak field case, these systems have a pronounced inert He core plus a weakly bound electronlike structure. Stronger fields lead more compact systems unless the stability is lost due to level crossings.

DOI: 10.1103/PhysRevA.89.052501 PACS number(s): 32.10.Ee

I. INTRODUCTION

The solution of Coulombic few-body problems plays a central role in testing the accuracy of quantum mechanical calculations as well as in studying the electron correlation in strongly interacting systems. The addition of magnetic fields enriches the physics of these systems allowing the fine tuning of the binding and structure of properties. The interest in Coulombic systems in magnetic field is further enhanced by the discovery of the strong magnetic field of white dwarfs [1,2] ($\approx 10^7$ G) and of neutron stars [3] ($\approx 10^{12}$ G). In the latest white dwarf catalog based on the Sloan digital sky survey data release 7 521, hydrogen-rich white dwarf stars have been listed [4]. Accurate calculations of wavelengths and oscillator strengths for hydrogen and other atoms and molecules are needed to explain the observed spectra in the strong magnetic fields of these stars. Similar few-body problems exist in condensed matter physics, in systems of electrons and holes in quantum dots, where the small effective masses and the large dielectric constant lead to large effective magnetic fields [5–8].

The solution of these few-body problems is complicated. First of all, the magnetic field breaks the symmetry of the system and this symmetry breaking has to be taken into account in constructing the wave function. Second, the magnetic field confines the system in the plane perpendicular to the direction of the field leading to elongated structures. In these structures, the competition between the Coulomb interaction and the magnetic field determines the energy levels of the system and the correlation between the particles. At very strong fields, the magnetic field dominates, e.g., the spins are aligned antiparallel to the direction of the field and the spin-flip energy is much larger than the single-particle energy, at weak fields the Coulomb interaction has more pronounced effect, but there is no perturbative regime where one or the other can be neglected.

Various computational methods have been developed to tackle the problem of calculation of energies of atoms and molecules in magnetic fields including the Hartree-Fock method [9], variational calculations with Gaussian [10,11], Hylleraas [12,13], or Lagrange basis functions [14], quantum Monte Carlo [15,16], and finite-element calculations [17]. Most of these approaches treat all electrons explicitly, but some introduce approximations restricting the core electron degrees of freedom to reduce the computational burden [18].

The simplest system, the one-electron problem, has been intensively studied using B-splines [19], finite elements [17], power series [20], and Lagrange mesh [21] methods, and the properties of the hydrogen atom in magnetic field are accurately known. The two electron systems, including the He atom [14,22–28] and the H$^-$ ion [29–37], have been also the focus of numerous studies and serve as a benchmark test for quantum mechanical calculations.

The number of calculations for three-electron systems is much less. Ivanov and Schmelcher studied the Li atom in magnetic field using the Hartree-Fock method [38]. Variations of approaches restricting the core electrons [18,39] have also been used to solve this problem. The most accurate energies of this system are calculated by the Hylleraas approach [12].

The formation of the He$^-$ ion received considerable theoretical and experimental interest. The first variational calculation on He$^-$ dates back to the 1960s [40,41]; a great list of references of theoretical and experimental studies addressing the existence of He$^-$ can be found in Ref. [42]. At the level of nonrelativistic quantum mechanics, the He$^-$ ion has two bound excited states, $1s2s2p\ {}^4P^o$ and the $2p^3\ {}^4S^o$ [43,44], but the $1s^2 2s\ {}^1S^e$ ground state is not bound. The double excited $1s2s2p\ {}^4P^o$ and the triple excited $2p^3\ {}^4S^o$ state are only bound in the nonrelativistic framework where spin and the angular momentum is conserved. At the level of full relativistic Hamiltonian, these states are metastable, and they decay by autoionizing to the adjacent continua via the spin-dependent relativistic forces.

The He$^-$ ion in an external field is of particular interest, because of the prediction that any anion in a magnetic field has infinitely many bound states [45,46] and the He$^-$ ion could be one of the simplest examples of that. This prediction motivated several studies to calculate the energy of He$^-$ in magnetic field [13,32,33,47]. Using a model Hamiltonian, which is capable to describe the binding mechanism in weak fields, Refs. [32,33,46] predict the existence of He$^-$ and other negative ions [30,31] in magnetic field. In Ref. [47], the multiconfiguration interaction approach is used to calculate the effects of strong magnetic fields on the excited states of the He$^-$ ion. This approach uses linear combinations of He core plus valence electron-type basis functions and proved to be accurate in comparing to benchmark calculations. A recent work [13] uses a single Hylleraas-type basis function modified by a Gaussian factor and the accuracy of the approach, compared to benchmark results, is limited to about 0.01 a.u.

In this paper, we will calculate the energy of He$^-$ ion in magnetic field using the stochastic variational method [11] with an explicitly correlated Gaussian (ECG) basis [10]. Variational calculations using ECGs proved to be extremely accurate in predicting binding energies and other properties in few-particle systems including the stability domains [10,48,49]. The main advantage of the ECG basis is that the matrix elements are analytically available, and by increasing the number of basis states the accuracy can be enhanced.

In this study, we will systematically investigate all states with total spin angular momentum $S = \frac{1}{2}, \frac{3}{2}$ and magnetic quantum numbers $M = 0, -1, -2, -3$. As noted above, two of these states are bound without magnetic field, and other states become bound at certain values of the magnetic field strength, or not bound at all.

The outline of this paper is as follows. After the Introduction, the paper gives a brief overview of the method. The energy levels and structure of He$^-$ are investigated in Sec. III, followed by the conclusion in Sec. IV.

II. FORMALISM

A. Hamiltonian

We assume that the nucleus is infinitely heavy and it is at the origin of the coordinate system. The Hamiltonian of a Coulombic N-particle system in magnetic field is defined as

$$H = \sum_{i=1}^{N} \left(-\frac{1}{2}\Delta_i + \frac{B^2}{8}(x_i^2 + y_i^2) - \frac{Z}{r_i} \right) + \sum_{i<j}^{N} \frac{1}{r_{ij}} + \frac{B}{2}(L_z + 2S_z) \tag{1}$$

$$= T + V_{ho} + V_{Ne} + V_{ee} + \frac{B}{2}(L_z + 2S_z), \tag{2}$$

where L_z (S_z) is the z component of the orbital momentum (spin) of the system, the magnetic field of strength B is directed along the z axis, and Z is the charge of the nucleus. In the second part of the equation, we separated the terms of the Hamiltonian into kinetic energy (T), two-dimensional harmonic-oscillator-like contribution of the magnetic field (V_{ho}), plus the Coulomb interaction between the electrons (V_{ee}) and between the nucleus and the electrons (V_{Ne}). The positions of the particles are denoted by $\mathbf{r}_i = (x_i, y_i, z_i)$, and the relative distances are defined by $\mathbf{r}_{ij} = \mathbf{r}_i - \mathbf{r}_j$. Atomic units are used, and the magnetic field in these units is equal to 2.35×10^9 G times B.

B. Basis functions

The variational method will be used to calculate the energy of the system. As a trial function, we choose a deformed form of the correlated Gaussians [10,11]:

$$\exp\left\{ -\frac{1}{2}\sum_{i,j=1}^{N} A_{ij}\rho_i\rho_j - \frac{1}{2}\sum_{i,j=1}^{N} B_{ij} z_i z_j \right\}, \tag{3}$$

where the nonlinear parameters are different (and independent) in the "xy" and "z" directions, and $\rho_i = (x_i, y_i)$. This extension brings a great deal of flexibility by allowing a separate description on the "xy" plane and along the "z" axis. The Hamiltonian does not commute with L^2 but it has common eigenfunctions with L_z. The above form of the deformed correlated Gaussian (DCG) belongs to quantum number $M = 0$. To allow for $M \neq 0$ states, we multiply the basis by

$$\prod_{i=1}^{N} \xi_{m_i}(\rho_i), \tag{4}$$

where

$$\xi_m(\rho) = (x + iy)^m. \tag{5}$$

Thus, our variational trial function reads as

$$\Phi_M(\mathbf{r}) = \mathcal{A}\left(\prod_{i=1}^{N} \xi_{m_i}(\rho_i) \right) \times \exp\left\{ -\frac{1}{2}\sum_{i,j=1}^{N} A_{ij}\rho_i\rho_j - \frac{1}{2}\sum_{i,j=1}^{N} B_{ij} z_i z_j \right\}, \tag{6}$$

where m_i are integers and $M = m_1 + m_2 + \ldots + m_N$. This function is coupled with the spin function χ_{SS_z} to form the trial function ($S_z = -S$ used in the calculations). If several intermediate spin couplings exist, each function is included as a separate variational trial function. We restrict ourselves to positive parity states $\Pi_z = 1$ in nonzero magnetic field calculations. The trial function should be multiplied by z-dependent factors to account for negative parity states. In a magnetic field, the conserved quantum numbers are M, Π_z, S^2, and S_z. The quantum states in a magnetic field are often denoted by $\nu_{S_z}^{2S+1} M^{(-1)^{\Pi_z}}$, where ν is the degree of excitation. In our case, only M and S will be changed and we can characterize the states with these two quantum numbers. Note that in the field-free case L^2 is a good quantum number and the notation of the states is $n_{S_z}^{2S+1} L_M$.

The DCG basis function can be rewritten in an equivalent form which emphasizes the distance between particles

$$\exp\left\{ -\frac{1}{2}\sum_{i,j=1}^{N} A_{ij}\rho_i\rho_j - \frac{1}{2}\sum_{i,j=1}^{N} B_{ij} z_i z_j \right\} = \exp\left\{ -\frac{1}{2}\sum_{i,j=1}^{N} \alpha_{ij}(\rho_i - \rho_j)^2 - \frac{1}{2}\sum_{i,j=1}^{N} \beta_{ij}(z_i - z_j)^2 - \frac{1}{2}\sum_{i=1}^{N} \alpha_i' \rho_i^2 - \frac{1}{2}\sum_{i=1}^{N} \beta_i' z_i^2 \right\}. \tag{7}$$

The new parameters α_{ij}, β_{ij}, α_i', and β_i' can be defined in terms of A_{ij} and B_{ij} [10,11]. The variational parameters α_{ij} and β_{ij} are related to the pair distances between the electrons, and the parameters α_i' and β_i' are defined by the distance between the nucleus and the electrons. We can select these parameters from a $[\gamma_{\min}, \gamma_{\max}]$ interval; $\gamma_{\min}$ will determine the closest distance between particles and $\gamma_{\max}$ defines the maximum distance. For a weakly bound state, $\gamma_{\max}$ is chosen to allow the particles to be far away from the nucleus.

The ECGs are very widely used in atomic physics and quantum chemistry [10]. The main advantages of ECG bases are as follows: (1) their matrix elements are analytically

TABLE I. Energy and matrix elements of the ($M=-1, S_z=-\frac{1}{2}$) He$^-$ in magnetic field ($B=0.8$ a.u.). The energy E is the sum of the kinetic and potential energies plus $\frac{B}{2}(M+2S_z)$. All quantities are given in atomic units.

N	E	η	$\langle T\rangle$	$\langle V_{ee}\rangle$	$\langle V_{Ne}\rangle$	$\langle V_{ho}\rangle$
50	−2.812637	0.999949	3.474194	1.704295	−7.678430	0.487304
100	−2.814422	0.999966	3.475614	1.700966	−7.678344	0.487042
200	−2.814755	0.999976	3.475687	1.700918	−7.678422	0.487018
400	−2.814941	0.999999	3.476127	1.700147	−7.678280	0.487065

available for a general N-particle system, (2) they are flexible enough to approximate rapidly changing functions, (3) the permutation symmetry can be easily imposed, and (4) one can make a simple transformation between single-particle and relative coordinate systems [10,11].

The basis parameters can be efficiently chosen by the stochastic variational method (SVM) [10,11]. In this approach, the variational parameters A_{ij} and B_{ij} of the DCG basis [see Eq. (6)] are randomly selected and the parameters giving the lowest variational energy are retained as basis states. This procedure can be fine tuned into an efficient optimization scheme as described in details in Refs. [10,11].

Despite the computational advantages, the ECG basis was regarded as inferior to the exponential $\exp(-\alpha r)$ form since the ECG basis functions do not have the correct functional form near the $r_{ij}\to 0$ coalescence point for Coulomb interactions. They also have the incorrect forms for the $r_{ij}\to\infty$ asymptote for short-range potentials. To investigate this issue, we have compared the local properties and accuracy of the ground-state wave functions obtained by the stochastic variational method with ECG basis to the direct solution of the Schrödinger equation calculated by the correlation-function hyperspherical-harmonic method (CFHHM) [50]. A Coulombic three-particle system, the Ps$^-$ ion was used as an example and the ground-state energies agreed to up to 10 digits. To compare the local properties, we have evaluated the amplitudes of the values of the operator $D=H\Psi/E\Psi-1$, characterizing the local deviation of the wave function from its true value. We have found that the D values calculated by SVM are consistently larger (by up to five orders of magnitude) than in the CFHHM. Despite this, the SVM observables, except $\langle\delta(r_k)\rangle$, converge to significantly more digits than the CFHHM observables for their respective selected bases. In other words, a sufficiently large ECG basis provides a very accurate description of the energy and the observables despite the inaccuracy in the the local properties of the wave function. Moreover, the shortcomings of the ECG basis are greatly compensated by the speed and simplicity of matrix element calculations. Due to these advantages, ECG-based variational calculations became the method of choice describing a number of diverse physical systems.

Reference [10] provides a thorough review of the applications of the ECG basis in various problems. Benchmark tests presented for $N=2$–5 electron atoms show that the ECG basis can produce up to 10-digit accuracy for 2–3 electron atoms, and while for 2–3 electron atoms the Hylleraas basis is more accurate, for $N=4$–5 particles only the ECG basis seems to be feasible. The ECG basis also proved to be very accurate in calculating weakly bound states. A series of positronic atoms have been predicted using the stochastic variational method with ECG basis [50–57]. The binding energy in these systems [10] ranges from 0.001 to 0.04 a.u. and these weakly bound states with complicated clustering structures can be accurately described with the ECG basis.

C. Observables

To investigate the stability, we will compare the one-particle ionization threshold energy $E_T(M,S_z)$ (the energy needed to move one electron to infinity) to the energy of the He$^-$ ion. The system is stable if the total energy is lower than the threshold energy, which is defined as

$$E_T(M,S_z)=\min_{M^{\rm He},S_z^{\rm He}}\left[E^{\rm He}\left(M^{\rm He},S_z^{\rm He}\right)+E^e\left(M^e,S_z^e\right)\right], \quad (8)$$

where $E^{\rm He}(M^{\rm He},S_z^{\rm He})$ is the total energy of the He atom, and

$$E^e\left(M^e,S_z^e\right)=\left(M^e+|M^e|+2S_z^e+1\right)\frac{B}{2} \quad (9)$$

is the energy of the Landau levels of the electron. The quantum numbers satisfy

$$M=M^{\rm He}+M^e,\qquad S_z=S_z^{\rm He}+S_z^e. \quad (10)$$

Here, we emphasize again that these states are only bound in the nonrelativistic framework, but will become metastable when a relativistic Hamiltonian is used.

Aside from these energies, we will also calculate the probability density and the average distances between particles. The probability density averaged over the radial coordinate is defined as

$$C(z)=\langle\Psi|\sum_i\delta(z-z_i)|\Psi\rangle, \quad (11)$$

TABLE II. Energies (in a.u.) of the ${}^4S^o$ and ${}^4P^o$ states He$^-$. $N=800$ basis functions are used.

	This work	Literature	η	r_{ee}^2	r_{Ne}^2
He$^-$ ${}^4P^o$	−2.178077440	−2.17807725 [61]	0.99999955	116.16	52.39
He$^-$ ${}^4S^o$	−0.723058734	−0.723058726 [61]	0.99999997	57.89	27.63

TABLE III. Energies (in a.u.) of He and He$^-$ in magnetic field.

	This work	Literature	η	ρ^2_{ee}	z^2_{ee}	ρ^2_{Ne}	z^2_{Ne}
He ($M=0, S_z=-1$)	-2.185038		0.99999996	8.18	4.09	4.08	2.04
He$^-$($M=-2, S_z=-\frac{3}{2}$)	-2.185286	-2.185216 [47]	1.00002	194.84	184.35	390.81	370.94

where Ψ is the variational wave function and the bra-ket notation stands for integration over all single-particle coordinates. Similarly,

$$C(\rho) = \langle\Psi|\sum_i \delta(\rho-\rho_i)|\Psi\rangle \tag{12}$$

is the probability distribution for the radial variable. Using these functions, the square distances are defined as

$$\rho^2_{Ne} = \int_0^\infty \rho^2 C(\rho) d\rho \tag{13}$$

and

$$z^2_{Ne} = \int_{-\infty}^{\infty} z^2 C(z) dz. \tag{14}$$

The pair distances are defined similarly, replacing the single-particle variables with the pair variables in the above equations. Distances between particles in a bound system are small and the particles are confined into distance of a few atomic units. Loosely bound systems tend to be larger, up to few tens on atomic units, but still finite. In unbound systems, the distances diverge.

D. Virial theorem

If the wave function is an exact eigenstate, it must satisfy the condition

$$\langle\Psi|[H,O]|\Psi\rangle = 0, \tag{15}$$

where O is any operator. In particular, if

$$O = \frac{i}{\hbar}\sum_i \mathbf{r}_i\mathbf{p}_i = \sum_i \mathbf{r}_i\frac{\partial}{\partial\mathbf{r}_i}, \tag{16}$$

then in the case of our Hamiltonian of Eq. (2) the virial theorem is

$$-2\langle\Psi|T|\Psi\rangle = \langle\Psi|V_{ee}+V_{Ne}|\Psi\rangle - 2\langle\Psi|V_{ho}|\Psi\rangle \tag{17}$$

or, by defining

$$\eta = -2\frac{\langle\Psi|T|\Psi\rangle}{\langle\Psi|V_{ee}+V_{Ne}|\Psi\rangle - 2\langle\Psi|V_{ho}|\Psi\rangle}, \tag{18}$$

the virial theorem is satisfied if $\eta = 1$. The virial theorem holds for the exact wave function, as well as for some approximate ones, but generally it is not fulfilled if finite basis sets are used. Checking how close the virial ratio η is to the ideal value 1 gives a useful measure of the quality of the wave function (the quality of the basis). However, the value $\eta = 1$ is only a necessary but not sufficient condition for the wave function to be accurate. One may obtain the exact value $\eta = 1$ for bad wave functions by scaling [58]. In our approach, we will calculate the virial factor as a function of the basis size. We will show that using the SVM, both the energy and the virial factor converge and the wave function is improved in the optimization procedure.

TABLE IV. Energies (in a.u.) of $M = 0$, $S_z = -\frac{1}{2}$ Li in magnetic field. The estimation of Ref. [13] is –7.455 for $B = 0$ (in a.u.).

B	This work	Ref. [12]	ρ^2_{ee}	z^2_{ee}	ρ^2_{Ne}	z^2_{Ne}
0.0	-7.47804	-7.47806	8.18	4.09	4.08	2.04
0.1	-7.51405	-7.51405	6.98	4.02	3.47	2.00
0.5	-7.52393	-7.52392	3.17	4.63	1.57	2.31
1.0	-7.45542	-7.45428	1.80	6.24	0.89	3.11

III. RESULTS

In the following, we present some test calculations and then turn to the study of the binding of He$^-$ in magnetic field. $N = 400$ basis are states used in all calculations unless otherwise noted. Each calculation is started from scratch, that is, the basis functions are optimized for each case independently. Our experience is that a basis function set that is optimized for a given magnetic field can be quite inaccurate when used for a different field, even if the field strengths are close.

A. Accuracy

We have made a series of test calculations to demonstrate that our approach is accurate enough to describe the He$^-$ ion in magnetic field. Our previous studies of few-particle systems in magnetic field [5–8,10,59,60] already show the reliability of the approach. Here, we show that the method is also accurate for weakly bound three-electron systems.

As a first test, we study the convergence of the energy and the virial factor as a function of basis size. Table I shows the average kinetic and potential energies and the virial factor. By increasing the basis size (N), the matrix elements converge to their variational estimates. At $N = 400$, the matrix elements are accurate up to five decimal values; by further increasing the basis dimension, the first five digits of the energy do not change. At the same time, the virial factor also converges to one up to five digits.

TABLE V. Energies (in a.u.) of $M = -1$, $S_z = -\frac{1}{2}$ Li in magnetic field. The estimation of Ref. [13] is –7.406 for $B = 0.0$ and –7.701 for $B = 1.0$ (in a.u.).

B	This work	Ref. [12]	ρ^2_{ee}	z^2_{ee}	ρ^2_{Ne}	z^2_{Ne}
0.0	-7.41003	-7.41016	14.81	3.80	7.39	1.89
0.1	-7.48734	-7.48734	10.60	3.13	5.28	1.56
0.5	-7.63693	-7.63693	4.09	1.71	2.01	0.85
1.0	-7.71913	-7.71836	2.50	1.22	1.20	0.60

TABLE VI. Energies (in a.u.) of $M = -3$, $S_z = -\frac{3}{2}$ Li in magnetic field. The estimation of Ref. [13] is –6.567 for $B = 1.0$ (in a.u.).

B	This work	Ref. [12]	ρ_{ee}^2	z_{ee}^2	ρ_{Ne}^2	z_{Ne}^2
0.0	−5.14264	−5.14232	195.89	25.04	96.96	12.42
0.1	−5.34116	−5.34103	34.02	6.29	14.66	3.09
0.5	−5.98232	−5.98225	10.47	2.76	4.39	1.35
1.0	−6.58255	−6.58236	6.12	1.96	2.55	0.95

As a second test, we have calculated the binding energies of the two bound states of He$^-$. Our results, presented in Table II, are slightly better than the best variational calculation [61]. The binding energy of the $^4P^o$ state of He$^-$ is very small (0.0028 a.u.), and this leads to a very large square radius and large square average electron-electron distance.

As third test, we have calculated the binding energy of the $(M = -2, S_z = -\frac{3}{2})$ state of He$^-$. This energy is calculated in Ref. [47] and found to be 0.00018 a.u. This is a very small binding energy and it is a stringent test of the approach for weakly bound states. The results presented in Table III are in good agreement with the results of Ref. [47] and improves the binding energy to 0.00025 a.u. The virial theorem is accurately satisfied. The structure of this state can be described as a very distant electron weakly bound to the He core.

Finally, we show the accuracy of the approach by calculating the energies of the Li atom in different magnetic fields and compared to the best value found in the literature (see Tables IV, V, and VI). Just as in other previous applications of the ECG basis for magnetic systems [10,60], the calculated energies agree with the previously published results proving the accuracy of the method.

Our results for the Li atom with no magnetic field (Tables IV, V, and VI) are slightly worse than the Hylleraas calculation. The reason is that the DCG basis is a deformed basis, while the Hamiltonian of the Li atom without magnetic field is spherically symmetric. The DCG basis converges slowly in this case. By increasing the number of basis functions, as it is shown in Table II, our approach reproduces the best energies in the zero magnetic field case.

For nonzero magnetic fields, our calculation agrees with or improves the Hylleraas results. The improvement is particularly significant in stronger magnetic fields where the cylindrical symmetry becomes dominant. This slows down the convergence of the Hylleraas basis (higher angular momentum states are needed) and the cylindrical basis used in this work becomes more suitable for the calculation.

In the following, we present our calculations and compare it to Refs. [13,47]. The basis function used in Ref. [47] built up from core plus valencelike configuration interaction wave functions using Slater-type orbitals. Various core configurations are used providing flexibility with a relatively basis low dimension. The convergence of the calculation with respect to the addition of further states is carefully studied and the approach is proved to be accurate in comparing to benchmark calculations. Reference [13] uses a single Hylleraas-type basis function modified by a Gaussian factor. The main deficiency of the single basis function is that it is difficult to use it to approximate clustering of particles. As we will show later, many of the He$^-$ configurations are a system of He core plus a loosely bound electron. As a benchmark test, the approach presented in Ref. [13] was used to calculate the energy of Li with and without magnetic field. The accuracy of the approach (see Tables IV, V, and VI) is limited.

Next, we will present our calculations for the $S = \frac{1}{2}, \frac{3}{2}$ and $M = 0, -1, -2, -3$ states. There are four bound states: $(M = -1, S_z = -\frac{1}{2})$, $(M = -1, S_z = -\frac{3}{2})$, $(M = -2, S_z = -\frac{3}{2})$, and $(M = -3, S_z = -\frac{3}{2})$. The other states $(M = 0, S_z = -\frac{1}{2})$, $(M = 0, S_z = -\frac{3}{2})$, $(M = -2, S_z = -\frac{1}{2})$, and $(M = -3, S_z = -\frac{1}{2})$ are predicted to be unbound. Out of these four unbound states we will show our results for the $(M = 0, S_z = -\frac{1}{2})$ case to illustrate how the calculation works for unbound systems. In the calculations presented below, the deviation of the virial factor from one is less than 10^{-5} and the energies are converged in all digits shown in the tables.

B. $M = 0$, $S_z = -\frac{1}{2}$ state

The $M = 0$, $S_z = -\frac{1}{2}$ state of He$^-$ is not bound. Note that in this case the energy of the He$^-$ should converge to the energy of the $M = 0$, $S_z = 0$ state of He. Table VII shows

TABLE VII. Energies (in a.u.) of $M = 0$, $S_z = -\frac{1}{2}$ He$^-$ in magnetic field are shown, as well as their respective threshold energies. The square of electron-electron distances in the radial and perpendicular directions ρ_{ee}^2 and z_{ee}^2, as well as the square of the electron-nucleus distances ρ_{Ne}^2 and z_{Ne}^2, are shown.

			He$^-$ $M = 0$, $S_z = -1/2$				
	Total energy		Threshold	Distances			
B	This work	Ref. [13]	$E_T = E^{\mathrm{He}}(M^{\mathrm{He}} = 0, S_z^{\mathrm{He}} = 0)$	ρ_{ee}^2	z_{ee}^2	ρ_{Ne}^2	z_{Ne}^2
0.00	−2.90292		−2.90372 [24]	875.85	243.06	437.89	121.52
0.10	−2.90108	−2.871	−2.90174 [14]	14.44	957.20	7.20	478.58
0.16	−2.89792	−2.861	−2.89829 [22]	9.42	897.28	4.70	448.61
0.24	−2.89169	−2.848	−2.89240 [14]	6.62	994.59	3.29	497.27
0.40	−2.87230	−2.816	−2.87287 [14]	4.36	1255.59	2.17	627.77
0.50	−2.85566	−2.794	−2.85624 [24]	3.67	1203.83	1.82	601.89
0.80	−2.78782	−2.713	−2.78843 [14]	2.58	1191.26	1.28	595.61
1.00	−2.72976	−2.652	−2.73037 [14]	2.19	1261.02	1.08	630.49
1.60	−2.50821		−2.50881 [14]	1.55	1260.54	0.77	630.26

TABLE VIII. Energies (in a.u.) of $M=-1$, $S_z=-\frac{1}{2}$ He$^-$ in magnetic field are shown, as well as their respective threshold energies. The square of electron-electron distances in the radial and perpendicular directions ρ_{ee}^2 and z_{ee}^2, as well as the square of the electron-nucleus distances ρ_{Ne}^2 and z_{Ne}^2, are also shown.

	He$^-$ $M=-1$, $S_z=-1/2$						
	Total energy		Threshold	Distances			
B	This work	Ref. [13]	$E_T = E^{\mathrm{He}}(M^{\mathrm{He}}=0, S_z^{\mathrm{He}}=0)$	ρ_{ee}^2	z_{ee}^2	ρ_{Ne}^2	z_{Ne}^2
0.00	−2.90330		−2.90372 [24]	5084.60	312.76	2542.26	156.37
0.10	−2.90196	−2.892	−2.90174 [14]	27.56	232.45	13.74	116.19
0.16	−2.89955	−2.905	−2.89829 [22]	17.54	114.85	8.72	57.39
0.24	−2.89495	−2.904	−2.89240 [14]	11.99	54.55	5.93	27.24
0.40	−2.88081	−2.899	−2.87287 [14]	7.58	20.45	3.70	10.18
0.50	−2.86844	−2.887	−2.85624 [24]	6.27	14.44	3.03	7.18
0.80	−2.81494	−2.836	−2.78843 [14]	4.28	7.27	2.03	3.59
1.00	−2.76657	−2.794	−2.73037 [14]	3.59	5.51	1.69	2.71
1.60	−2.57177	−2.658	−2.50881 [14]	2.49	3.44	1.15	1.68

that our calculation indeed converges to that threshold. The convergence could be further improved by increasing the range of the Gaussians, allowing a better approximation of the wave function as a bound He and an electron in the continuum. The results of Ref. [13] are only close to the threshold in the case of weak fields and very far off in stronger field cases.

The $M=0$, $S_z=-\frac{1}{2}$ state of He$^-$ is analogous to the $M=0$, $S_z=-\frac{1}{2}$ state of Li, but the latter is strongly bound (the ionization energy is about 0.2 a.u. at $B=0$ and it increases with the magnetic field). The squares of electron-electron ρ_{ee}^2 (z_{ee}^2) and the electron-nucleus ρ_{Ne}^2 (z_{Ne}^2) distances in the radial (perpendicular) direction are also shown in Table VII. The harmonic oscillator part of the Hamiltonian confines the particles in the radial direction, so the ρ_{ee}^2 and ρ_{Ne}^2 distances are finite and decreasing with increasing magnetic field. In the perpendicular direction, z_{ee}^2 and z_{Ne}^2 diverge showing that an electron is detached from the He atom. By increasing the range of the Gaussians (γ_{max}) in the basis functions, these distances increase. The results presented in Table VII are calculated with $\gamma_{\mathrm{max}}=100$.

C. $M=-1$, $S_z=-\frac{1}{2}$ state

Reference [13] predicts the existence of a bound $M=-1$, $S_z=-\frac{1}{2}$ state of He$^-$ in the 0.16 a.u. $\leqslant B \leqslant$ 0.8 a.u. magnetic field region. Our calculation confirms that this state is indeed bound, but the binding energy and the stability region are quite different from the ones predicted in Ref. [13]. The He plus electron threshold of this state is equal to the energy $E^{\mathrm{He}}(M^{\mathrm{He}}=0, S_z^{\mathrm{He}}=0)$ of the He atom in magnetic field since the contribution of the electron is $E^e(M^e=-1, S_z^e=-\frac{1}{2})=0$. Reference [13] uses the energy of the $(M^{\mathrm{He}}=-1, S_z^{\mathrm{He}}=-1)$ state of the He atom as a threshold for larger magnetic field ($B>0.8$ a.u). This is wrong because the energy of the electron $[E^e(M^e=0, S_z^e=\frac{1}{2})=B]$ has to be added to get the correct value, which is above the energy of the $(M^{\mathrm{He}}=0, S_z^{\mathrm{He}}=0)$ state of He. Therefore, $E^{\mathrm{He}}(M^{\mathrm{He}}=0, S_z^{\mathrm{He}}=0)$ is the threshold.

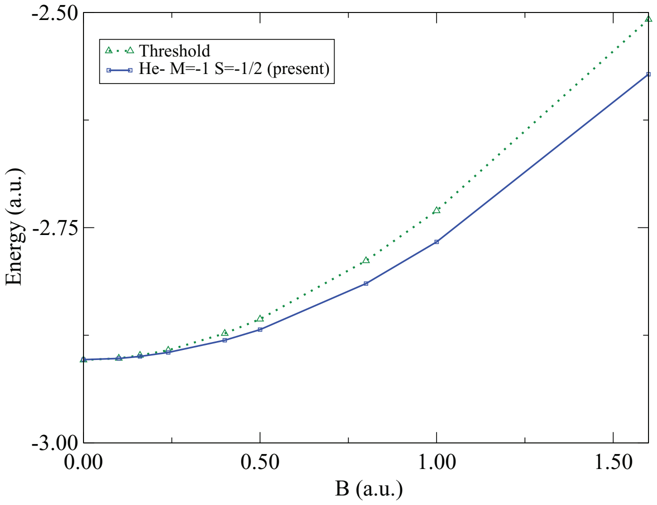

FIG. 1. (Color online) Energies of the $M=-1$, $S_z=-\frac{1}{2}$ state of He$^-$ for different magnetic field intensities. The threshold energies are also shown.

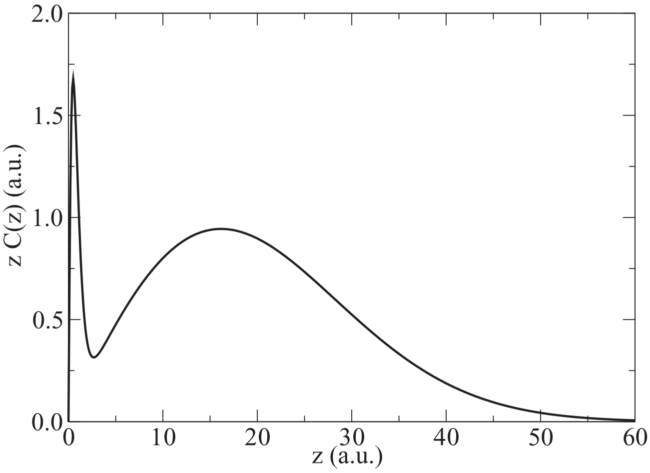

FIG. 2. Probability density averaged over the radial coordinate and multiplied by z of the $M=-1$, $S_z=-\frac{1}{2}$ state of He$^-$ in a magnetic field $B=0.1$ a.u.

TABLE IX. Energies (in a.u.) of $M = -1$, $S_z = -\frac{3}{2}$ He$^-$ in a magnetic field B are shown, as well as their respective thresholds. The threshold energies are associated with state $E^{\rm He}(M^{\rm He} = 0, S_z^{\rm He} = -1)$ for $B < 0.1$ a.u.. At $B = 0.1$ a.u. and above they are associated with $E^{\rm He}(M^{\rm He} = -1, S_z^{\rm He} = -1)$ instead. Calculated thresholds were obtained using Eq. (8) employing the values of $E^{\rm He}$ found in the respective cited sources. The square of electron-electron distances in the radial and perpendicular directions ρ_{ee}^2 and z_{ee}^2, as well as the square of the electron-nucleus distances ρ_{Ne}^2 and z_{Ne}^2, are also shown.

He$^-$
$M = -1$, $S_z = -3/2$

	Total energy		Threshold	Distances			
B	This work	Ref. [47]	E_T	ρ_{ee}^2	z_{ee}^2	ρ_{Ne}^2	z_{Ne}^2
0.00	−2.17802	−2.178017	−2.17522 [14]	88.46	23.53	39.18	11.11
0.02	−2.21360	−2.213567	−2.19447 [14]	61.14	18.09	25.77	8.42
0.04	−2.24352	−2.243481	−2.21225 [62]	48.87	16.05	20.18	7.42
0.06	−2.26980	−2.269752	−2.22869 [62]	41.12	14.86	16.82	6.83
0.08	−2.29347	−2.293392	−2.24397 [62]	35.58	14.19	14.50	6.50
0.10	−2.31516	−2.315028	−2.26142 [62]	31.34	13.78	12.76	6.30
0.14	−2.35421	−2.353990	−2.30464 [62]	25.23	13.49	10.29	6.14
0.20	−2.40571	−2.404995	−2.36470 [62]	19.32	14.04	7.94	6.38
0.40	−2.55323		−2.54076 [23]	9.86	27.28	4.30	12.91
0.50	−2.62430		−2.62002 [23]	7.53	55.81	3.43	27.25
0.80	−2.83436		−2.83562 [23]	4.59	365.59	2.22	182.60
1.00	−2.96468		−2.96550 [23]	3.80	894.17	1.83	446.95

The energy of the $M = -1$, $S_z = -\frac{1}{2}$ state of He$^-$ is shown in Table VIII and in Fig. 1. According to our calculation, this state is stable in a magnetic field starting at around $B = 0.01$ a.u. and remains stable with increasing magnetic field. The calculation of the precise boundary of the stability region is computationally expensive (many basis functions are required to represent the very weakly bound system).

Table VIII shows that the distances between particles (except for the unbound zero magnetic field case) are finite. A further check of the stability is that by increasing the range of the Gaussians ($\gamma_{\rm max}$), the distance between particles converges to the same number. This test corroborates that the state in the $B = 0.1$ a.u. magnetic field is a loosely bound state, with binding energy of 0.004 a.u.. This state is a system of a He atom with a loosely bound electron as it is shown in Fig. 2. The first, narrow peak of the probability density corresponds to the number of electrons of the He atom and the second, wide peak shows the position of the extra electron. Integrating this density up to 4 a.u. one gets about 2 corresponding to the He atom and one has to integrate up to 60 a.u. to account for the third electron.

The distances between the particles decrease as the magnetic field is increased, just as expected. The distances between the particles are somewhat larger than those of the $M = -1$, $S_z = -\frac{1}{2}$ state of Li (Table V) because the He$^-$ is less bound.

Energies calculated in Ref. [13] for magnetic field $B > 0.16$ a.u. are significantly below our variational results. We have shown the convergence of energy (see Table I) for $B = 0.8$ a.u. In this case, the energy calculated in Ref. [13] is below our accurate variational estimate by 0.02 a.u. The reason of this discrepancy is not clear. We speculate that the nine-dimensional numerical integration used in Ref. [13] may lead to the loss of the variational property, but further investigation is needed to settle this issue.

D. $M = -1$, $S_z = -\frac{3}{2}$ state

The energies of this state have been calculated in Ref. [47] and our results are in very good agreement (up to 3 decimals,

TABLE X. Energies (in a.u.) of $M = -2$, $S_z = -\frac{3}{2}$ He$^-$ in a magnetic field are shown, as well as their respective thresholds. The threshold energies are associated with the state $E^{\rm He}(M^{\rm He} = 0, S_z^{\rm He} = -1)$. At $B = 0.1$ a.u. and above, they are associated with $E^{\rm He}(M^{\rm He} = -1, S_z^{\rm He} = -1)$ instead. Calculated thresholds were obtained using Eq. (8) employing the values of $E^{\rm He}$ found in the respective cited sources. The square of electron-electron distances in the radial and perpendicular directions ρ_{ee}^2 and z_{ee}^2, as well as the square of the electron-nucleus distances ρ_{Ne}^2 and z_{Ne}^2, are also shown.

He$^-$
$M = -2$, $S_z = -3/2$

	Total energy		Threshold	Distances			
B	This work	Ref. [47]	E_T	ρ_{ee}^2	z_{ee}^2	ρ_{Ne}^2	z_{Ne}^2
0.01	−2.18529	−2.18522	−2.18504 [62]	194.84	184.35	390.81	370.94
0.02	−2.19572	−2.19560	−2.19447 [62]	200.51	151.66	96.80	74.52
0.08	−2.25398	−2.25313	−2.24397 [62]	26.95	16.64	58.93	36.31
0.10	−2.27108	−2.26962	−2.26142 [62]	48.64	32.16	22.23	14.50
0.20	−2.36053	−2.34009	−2.36470 [62]	10.26	126.74	21.11	255.48

TABLE XI. Energies (in a.u.) of $M=-3$, $S_z=-\frac{3}{2}$ He$^-$ in a magnetic field are shown, as well as their respective thresholds. The threshold energies are associated with the state $E^{\text{He}}(M^{\text{He}}=0,S_z^{\text{He}}=-1)$ for $B<0.1$. At $B=0.1$ a.u. and above they are associated with $E^{\text{He}}(M^{\text{He}}=-1,S_z^{\text{He}}=-1)$ instead. Calculated thresholds were obtained using Eq. (8) employing the values of E^{He} found in the respective cited sources. The square of electron-electron distances in the radial and perpendicular directions ρ_{ee}^2 and z_{ee}^2, as well as the square of the electron-nucleus distances ρ_{Ne}^2 and z_{Ne}^2, are also shown.

	He$^-$ M=−3, S_z=−3/2						
	Total energy		Threshold	Distances			
B	This work	Ref. [13]	E_T	ρ_{ee}^2	z_{ee}^2	ρ_{Ne}^2	z_{Ne}^2
0.00	−2.17291		−2.17522 [14]	2226.29	118.64	1110.17	59.14
0.10	−2.28622		−2.26142 [62]	58.87	16.98	23.66	8.16
0.16	−2.35635		−2.32519 [23]	39.04	12.98	15.72	6.23
0.24	−2.44064		−2.40239 [23]	27.35	10.52	11.10	5.04
0.40	−2.58982	−2.563	−2.54076 [23]	17.29	7.99	7.08	3.81
0.50	−2.67463	−2.650	−2.62002 [23]	14.12	7.08	5.80	3.38
0.80	−2.90436	−2.891	−2.83562 [23]	9.22	5.41	3.81	2.58
1.00	−3.04245	−3.034	−2.96550 [23]	7.54	4.77	3.11	2.27
1.60	−3.40705	−3.394	−3.30877 [23]	4.94	3.60	2.04	1.72

see Table IX) with that calculation. Reference [47] predicted that this state is bound with increasing magnetic fields. In that work, only the $E^{\text{He}}(M^{\text{He}}=0,S_z^{\text{He}}=-1)$ threshold was considered. Here, we show that the $(M=-1, S_z=-\frac{3}{2})$ states become bound in small nonzero magnetic field and it remains bound up to about $B<0.5$ a.u. At about $B=0.5$ a.u., the system becomes unbound with respect to the $E^{\text{He}}(M^{\text{He}}=-1,S_z^{\text{He}}=-1)$ threshold.

E. $M=-2$, $S_z=-\frac{3}{2}$ state

This state was also studied in Ref. [47] and predicted to be bound with increasing B. Similar to the previous case, only the $E^{\text{He}}(M^{\text{He}}=0,S_z^{\text{He}}=-1)$ threshold was considered, and this state becomes unbound with respect to the energy associated with the $E^{\text{He}}(M^{\text{He}}=-1,S_z^{\text{He}}=-1)$ state at about $B=0.2$ a.u. (see Tables III and X). Our calculation is in good agreement with the results of Ref. [47] for the bound states.

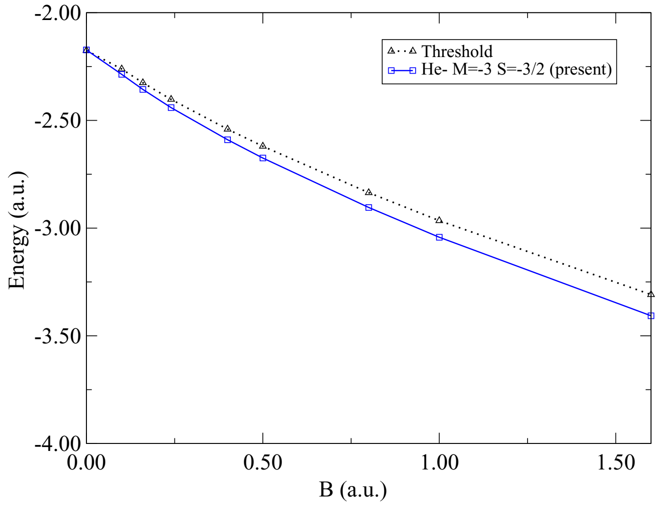

FIG. 3. (Color online) Energies of the $M=-3$, $S_z=-\frac{3}{2}$ state of He$^-$ for different magnetic field intensities. The threshold energies are also shown.

F. $M=-3$, $S_z=-\frac{3}{2}$ state

The $M=-3$, $S_z=-\frac{3}{2}$ state, corresponding to the loosely bound state of Li, with the same quantum numbers, is also bound (Table XI and Fig. 3). The relevant threshold is associated with the $(M^{\text{He}}=0,S_z^{\text{He}}=-1)$ state of He at $B<0.1$. At $B=0.1$ a.u. and above the threshold is determined by $E^{\text{He}}(M^{\text{He}}=-1,S_z^{\text{He}}=-1)$ [see Eq. (8)]. This He$^-$ state is much less bound than the analogous Li state (at $B=0.1$ a.u. the binding energy of He$^-$ is 0.02 a.u., that of Li is 0.14 a.u.), but as the energy and the particle-particle distances show the system is bound. The system becomes bound at small magnetic fields at about $B=0.02$ a.u. and remains stable with increasing magnetic field.

Reference [13] predicted that this state becomes bound at $B=0.7$ a.u. because the energy of the $M=-3$, $S_z=-\frac{3}{2}$ state of He$^-$ was compared to the energy of the $M=0$, $S_z=0$ state of the He atom (see Table VII for the energy of the latter state). This is, however, not correct because that violates the spin conservation in Eq. (10) so a decay into such state is not possible within the nonrelativistic framework.

IV. CONCLUSION

Using the stochastic variational method, we have calculated the energies of different states of the He$^-$ ion in a magnetic field. The calculations presented in this paper show that the deformed correlated Gaussian functions provide a flexible basis for variational calculations for atoms in magnetic fields. Using both the binding energy and the distances between the particles, we have confirmed the stability of He$^-$ for different quantum numbers. Our calculation is in good agreement with the calculation presented in Ref. [47] for weak magnetic fields. Our approach is more accurate than previous calculations, especially in the strong field cases where the cylindrical symmetry of the system can only be described by using higher angular momentum states in Hyllaraas calculations.

The accuracy of the present calculation for the three-electron system of the He$^-$ ion is still far worse than the accuracy of the field-free calculations. The accuracy can be increased by adding more basis functions, but the symmetry breaking caused by the magnetic field makes the convergence slower. Highly accurate calculations are needed to determine the stability domains and physical properties of the system as a function of magnetic field. Without improving the results of previous calculations, the structure of the system (e.g., the distances between particles) can not be reliably calculated because these quantities are very sensitive to the binding energy.

Aside from the astrophysical interest, the study of energy levels and wave function of three-electron atoms in a magnetic field is also important because it allows us to explore the electron correlations in a confined system in a tunable way. The electron-electron correlation depends both on the nuclear charge and on the strength of the magnetic field. By systematically changing these parameters, one can map the electron correlations. This can be used to construct exchange-correlation potentials or model Hamiltonians and it will also show the relative role of the Coulomb and harmonic oscillator potential in determining the wave function of the electrons. The results of these calculations are also important in condensed matter physics where the energy levels of few-electron quantum dots in external field can be measured and compared to calculations.

Accurate calculations serve not only as a benchmark test helping to improve the computational approaches, but can also be used to check analytical predictions and model Hamiltonians. For example, the effective Hamiltonian proposed in Refs. [32,33,46] can be fine tuned using the variational wave function and it might be extended to other systems. The present calculations corroborate the prediction of Refs. [32,33,46] that while the three-dimensional potential was not strong enough to maintain the bound state of the He$^-$ negative ion, the introduction of the magnetic field leads to a quasi-one-dimensional potential resulting in a weak binding. We have also shown that these systems are needlelike structures with two electrons close to the nucleus and the third electron smeared out in a long tail.

The accuracy and flexibility of the present approach for $N = 3$ shows that the calculation of $N = 4$-5-6 electron systems is also possible. The computational complexity grows with $N!$ due to the antisymmetrization and with N^2 due the evaluation of the matrix elements. The optimization of the basis will also be computationally more demanding but it should be manageable for a few more particles. In that respect, the present approach is unique because approaches using Hylleraas or other correlated basis functions can not be easily used for larger systems.

This work was restricted to even parity states with $M = 0, -1, -2, -3$. Several other bound states may exist, for example, the $1s2s2p^4P^o$ and the $2p^3\ {}^4S^o$ states are bound even without magnetic field. The study of those systems is left for future work. Another possible subject for future work is the study of the effect of finite nuclear mass on the binding energy of these systems.

ACKNOWLEDGMENT

The authors wish to thank B. G. Cook for helpful discussions and careful reading of the manuscript.

---

[1] J. C. Kemp, J. B. Swedlund, J. D. Landstreet, and J. R. P. Angel, Astrophys. J. Lett. **161**, L77 (1970).

[2] J. R. P. Angel, E. F. Borra, and J. D. Landstreet, Astrophys. J. **45**, 457 (1981).

[3] J. Truemper, W. Pietsch, C. Reppin, W. Voges, R. Staubert, and E. Kendziorra, Astrophys. J. Lett. **219**, L105 (1978).

[4] B. Külebi, S. Jordan, F. Euchner, B. T. Gänsicke, and H. Hirsch, Astrophys. Astron. **506**, 1341 (2009).

[5] C. Riva, F. M. Peeters, and K. Varga, Phys. Rev. B **61**, 13873 (2000).

[6] C. Riva, F. M. Peeters, and K. Varga, Phys. Rev. B **63**, 115302 (2001).

[7] C. Riva, F. M. Peeters, and K. Varga, Phys. Rev. B **64**, 235301 (2001).

[8] K. Varga, P. Navratil, J. Usukura, and Y. Suzuki, Phys. Rev. B **63**, 205308 (2001).

[9] O.-A. Al-Hujaj and P. Schmelcher, Phys. Rev. A **70**, 033411 (2004).

[10] J. Mitroy, S. Bubin, W. Horiuchi, Y. Suzuki, L. Adamowicz, W. Cencek, K. Szalewicz, J. Komasa, D. Blume, and K. Varga, Rev. Mod. Phys. **85**, 693 (2013).

[11] Y. Suzuki and K. Varga, *Stochastic Variational Approach to Quantum-Mechanical Few-Body Problems* (Springer, Berlin, 1998).

[12] Y. Tang, L. Wang, X. Song, X. Wang, Z.-C. Yan, and H. Qiao, Phys. Rev. A **87**, 042518 (2013).

[13] A. V. Turbiner and J. C. Lopez Vieyra, Phys. Rev. Lett. **111**, 163003 (2013).

[14] M. Hesse and D. Baye, J. Phys. B: At., Mol. Opt. Phys. **37**, 3937 (2004).

[15] S. Boblest, C. Schimeczek, and G. Wunner, Phys. Rev. A **89**, 012505 (2014).

[16] C. Schimeczek, S. Boblest, D. Meyer, and G. Wunner, Phys. Rev. A **88**, 012509 (2013).

[17] C. Schimeczek and G. Wunner, Comput. Phys. Commun. **185**, 614 (2014).

[18] H. Qiao and B. Li, Phys. Rev. A **62**, 033401 (2000).

[19] L. B. Zhao and P. C. Stancil, Phys. Rev. A **77**, 035401 (2008).

[20] Y. P. Kravchenko, M. A. Liberman, and B. Johansson, Phys. Rev. A **54**, 287 (1996).

[21] D. Baye, M. Vincke, and M. Hesse, J. Phys. B: At., Mol. Opt. Phys. **41**, 055005 (2008).

[22] W. Becken, P. Schmelcher, and F. K. Diakonos, J. Phys. B: At., Mol. Opt. Phys. **32**, 1557 (1999).

[23] W. Becken and P. Schmelcher, J. Phys. B: At., Mol. Opt. Phys. **33**, 545 (2000).

[24] J.-J. Zhao, X.-F. Wang, and H.-X. Qiao, Chin. Phys. B **19**, 113102 (2010).

[25] W. Becken and P. Schmelcher, Phys. Rev. A **63**, 053412 (2001).

[26] W. Becken and P. Schmelcher, Phys. Rev. A **65**, 033416 (2002).

[27] O.-A. Al-Hujaj and P. Schmelcher, Phys. Rev. A **67**, 023403 (2003).

[28] O.-A. Al-Hujaj and P. Schmelcher, Phys. Rev. A **68**, 053403 (2003).
[29] O.-A. Al-Hujaj and P. Schmelcher, Phys. Rev. A **61**, 063413 (2000).
[30] V. G. Bezchastnov, P. Schmelcher, and L. S. Cederbaum, Phys. Rev. A **61**, 052512 (2000).
[31] V. G. Bezchastnov, L. S. Cederbaum, and P. Schmelcher, Phys. Rev. A **65**, 032501 (2002).
[32] V. G. Bezchastnov, P. Schmelcher, and L. S. Cederbaum, Phys. Rev. Lett. **95**, 113002 (2005).
[33] V. G. Bezchastnov, P. Schmelcher, and L. S. Cederbaum, Phys. Chem. Chem. Phys. **5**, 4981 (2003).
[34] V. G. Bezchastnov, L. S. Cederbaum, and P. Schmelcher, Phys. Rev. Lett. **86**, 5450 (2001).
[35] V. G. Bezchastnov, P. Schmelcher, and L. S. Cederbaum, Phys. Rev. A **65**, 042512 (2002).
[36] V. G. Bezchastnov, P. Schmelcher, and L. S. Cederbaum, Phys. Rev. A **75**, 052507 (2007).
[37] Z. Ji-Jun, W. Xiao-Feng, and Q. Hao-Xue, Chin. Phys. B **20**, 053101 (2011).
[38] M. V. Ivanov and P. Schmelcher, Phys. Rev. A **57**, 3793 (1998).
[39] X. Wang and H. Qiao, Phys. Rev. A **75**, 033421 (2007).
[40] A. W. Weiss, Phys. Rev. **122**, 1826 (1961).
[41] E. Holøien and S. Geltman, Phys. Rev. **153**, 81 (1967).
[42] D. M. Feldmann and F. W. King, J. Phys. B: At., Mol. Opt. Phys. **41**, 025002 (2008).
[43] C. A. Nicolaides, Y. Komninos, and D. R. Beck, Phys. Rev. A **24**, 1103 (1981).
[44] P. Kristensen, U. V. Pedersen, V. V. Petrunin, T. Andersen, and K. T. Chung, Phys. Rev. A **55**, 978 (1997).
[45] J. Avron, I. Herbst, and B. Simon, Commun. Math. Phys. **79**, 529 (1981).
[46] J. Avron, I. Herbst, and B. Simon, Phys. Rev. Lett. **39**, 1068 (1977).
[47] X. Guan, B. Li, and L. Wu, Phys. Rev. A **64**, 043402 (2001).
[48] S. Bubin, O. V. Prezhdo, and K. Varga, Phys. Rev. A **87**, 054501 (2013).
[49] E. Armour, J.-M. Richard, and K. Varga, Phys. Rep. **413**, 1 (2005).
[50] R. Krivec, V. B. Mandelzweig, and K. Varga, Phys. Rev. A **61**, 062503 (2000).
[51] S. Bubin and K. Varga, Phys. Rev. A **84**, 012509 (2011).
[52] J. Y. Zhang and J. Mitroy, Phys. Rev. A **76**, 014501 (2007).
[53] S. Bubin, M. Stanke, D. Kędziera, and L. Adamowicz, Phys. Rev. A **75**, 062504 (2007).
[54] K. Varga, Phys. Rev. Lett. **83**, 5471 (1999).
[55] J. Mitroy, Phys. Rev. A **72**, 032503 (2005).
[56] J. Mitroy, Phys. Rev. A **70**, 024502 (2004).
[57] J. Mitroy, J. At. Mol. Sci. **1**, 275 (2010).
[58] P.-O. Lwdin, J. Mol. Spectrosc. **3**, 46 (1959).
[59] K. Varga, in *Few-Body Problems in Physics 02*, Few-Body Systems, edited by R. Krivec, M. Rosina, B. Golli, and S. Sirca (Springer, Vienna, 2003), Vol. 14, pp. 191–195.
[60] K. Varga, Few-Body Syst. **47**, 65 (2010).
[61] M. Bylicki and G. Pestka, J. Phys. B: At., Mol. Opt. Phys. **29**, L353 (1996).
[62] The corresponding energy for helium was calculated in this work, using the same method, since it was not found in the literature.